
This is an electronic reprint of the original article.
This reprint may differ from the original in pagination and typographic detail.

Author(s): Pesola, M. & von Boehm, J. & Pöykkö, S. & Nieminen, Risto M.
Title: Spin-density study of the silicon divacancy
Year: 1998
Version: Final published version

Please cite the original version:

Pesola, M. & von Boehm, J. & Pöykkö, S. & Nieminen, Risto M. 1998. Spin-density study of the silicon divacancy. *Physical Review B*. Volume 58, Issue 3. 1106-1109. ISSN 1550-235X (electronic). DOI: 10.1103/physrevb.58.1106.

Rights: © 1998 American Physical Society (APS). This is the accepted version of the following article: Pesola, M. & von Boehm, J. & Pöykkö, S. & Nieminen, Risto M. 1998. Spin-density study of the silicon divacancy. *Physical Review B*. Volume 58, Issue 3. 1106-1109. ISSN 1550-235X (electronic). DOI: 10.1103/physrevb.58.1106, which has been published in final form at <http://journals.aps.org/prb/abstract/10.1103/PhysRevB.58.1106>.

All material supplied via Aaltodoc is protected by copyright and other intellectual property rights, and duplication or sale of all or part of any of the repository collections is not permitted, except that material may be duplicated by you for your research use or educational purposes in electronic or print form. You must obtain permission for any other use. Electronic or print copies may not be offered, whether for sale or otherwise to anyone who is not an authorised user.

Spin-density study of the silicon divacancy

M. Pesola

Laboratory of Physics, Helsinki University of Technology, FIN-02150 Espoo, Finland

J. von Boehm

Laboratory of Theoretical and Applied Mechanics, Helsinki University of Technology, FIN-02150 Espoo, Finland

S. Pöykkö and R. M. Nieminen

Laboratory of Physics, Helsinki University of Technology, FIN-02150 Espoo, Finland

(Received 9 March 1998)

The possible charge states of the silicon divacancy V_2 are studied using the local spin-density pseudopotential method. The ionic coordinates are relaxed without any symmetry constraints. We obtain the formation and binding energies as well as the ionization levels from total-energy calculations and use them to discuss several experiments. We find using the 216-atom-site supercell that V_2^0 and V_2^- have a ‘‘mixed’’ structure that includes both pairing and resonant-bond characters, V_2^0 being more of the pairing type and V_2^- more of the resonant-bond type. [S0163-1829(98)05327-2]

The Si divacancy V_2 is particularly attractive from the experimental point of view because it is easily produced by electron irradiation and is quite stable and immobile. However, the theoretical interpretation of the experimental results for V_2 has turned out to be a difficult task due to the existence of several low-energy (meta)stable ionic structures of V_2 . The reason for the difficulty is that formation of new bonds from the dangling-bond electrons of atoms surrounding V_2 may lead to a variety of competing ionic structures, such as a breathing-mode structure, a pairing Jahn-Teller (JT) structure (formation of weak covalent bonds¹⁻³) or a resonant-bond JT structure (the formation of two adjacent short bonds⁴⁻⁶).

The traditional linear-combination-of-atomic-orbitals model by Watkins and Corbett¹ (WC) for V_2 is based on the pairing of atoms 1 and 2 as well as 4 and 5 [see Fig. 1(a)]. The ideal nonrelaxed V_2^0 of D_{3d} symmetry has the doubly degenerate e_u [occupied by two electrons, see Fig. 1(b)] and e_g (unoccupied) states in the gap. The JT pairing distortion reduces the symmetry to C_{2h} causing the e_u and e_g levels to split to nondegenerate a_u , b_u and a_g , b_g levels, respectively. In the WC model V_2 undergoes a large JT distortion such that the a_g level falls lower to form two lowest gap levels with the b_u level [see Fig. 1(b)]. The WC model was constructed to explain the electron paramagnetic resonance (EPR) experiments including the hyperfine satellites, which indicate that the odd electron of the charged V_2^+ and V_2^- must have an amplitude on the mirror plane, and only the a_g and b_u states have this property.

The *ab initio* calculations by Saito and Oshiyama⁴ result in a different resonant-bond structure for V_2^- ($d_{23}=d_{13} < d_{12}$: $a_u^2 b_u^1$) and a pairing structure for V_2^+ ($d_{12} < d_{13} = d_{23}$: b_u^1), which has given rise to a discussion concerning the relevance of their results in interpreting the EPR data.^{7,8} Also, the *ab initio* calculations by Seong and Lewis⁵ give a resonant bond structure for V_2^0 ($d_{13}=d_{23} < d_{12}$: a_u^2). These calculations are based on the density-functional theory

(DFT) in the local-density (LD) approximation. However, spin-polarized DFT using the local spin density (LSD) approximation should be more appropriate for the cases where the defect has an odd number of electrons, i.e., V_2^+ and V_2^- .⁹ The present paper reports results from well-converged *ab initio* DFT LSD (and LD) calculations for all possible charge states of V_2 to obtain a conclusive and consistent description of this important defect.

Our calculations are performed using a self-consistent plane-wave pseudopotential method. The Vosko-Wilk-Nusair¹⁰ (VWN) and the Perdew-Zunger¹¹ (PZ) parametrizations of the Ceperley-Alder data¹² are used for the exchange-correlation energy.¹³ We use for silicon a first-principles norm-conserving pseudopotential¹⁴ in a fully separable Kleinman-Bylander form.¹⁵ The nonlinear core-valence corrections¹⁶ are used to account for the overlap of the core and the valence-electron charges. All calculations are done using a 15-Ry kinetic energy cutoff.

We have used a number of supercells of different sizes as

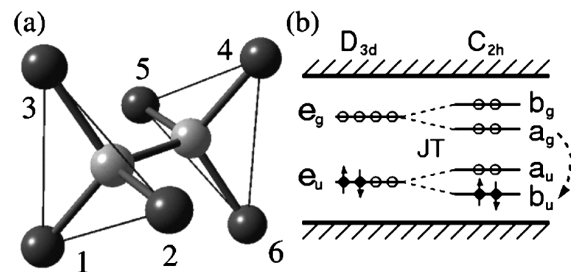


FIG. 1. (a) The atomic structure of the ideal divacancy with the six nearest-neighbor atoms. Dark spheres represent atoms, light gray spheres vacancies. (b) The effect of the Jahn-Teller pairing distortion on the levels of the silicon divacancy. The neutral charge state with two electrons in the gap level is shown. The arrow denotes lowering of the a_g level in positive and negative charge states suggested by Watkins and Corbett (Ref. 1). Occupation of defect levels in these two charge states is V_2^+ : a_g^1 and V_2^- : $a_g^2 b_u^1$ or V_2^+ : b_u^1 and V_2^- : $b_u^2 a_g^1$.

TABLE I. Ionization levels, formation (E_f), and binding energies (E_b) for the divacancy in Si (in eV). SC denotes the supercell.

	Γ , 216 SC	Γ , 128 SC	2^3 MP, 64 SC	Experiment
(0/+)	0.04	0.13	0.04	0.25 ^a
(-/0)	0.38	0.32	0.37	~ 0.55 ^b
(2-/-)	0.43	0.47	0.59	0.75 ^a
E_f (V_2^0)	4.94	4.38	5.65	
E_b (V_2^0)	1.60	1.90	1.19	≥ 1.6 ^a

^aEPR, Ref. 1.

^bPAS, Ref. 19.

well as different Brillouin zone (BZ) samplings to systematically explore the convergence of the computational results with respect to defect-defect interactions. Supercell sizes of 64, 128, and 216 atoms have been used. For the BZ sampling, the Γ point, the $\Gamma + L$, and the 2^3 Monkhorst-Pack¹⁷ (MP) k -point mesh have been used.

The ionic coordinates were relaxed without any symmetry constraints. The relaxation was continued until the largest remaining force component acting on any ion was less than 5 meV/Å. All calculations were performed in a massively parallel CRAY-T3E system using the FINGER code.¹⁸

The ionization level (Q'/Q) is defined as the position of the Fermi level μ_e above which the thermodynamically stable charge state of the divacancy changes from Q' to Q .

These levels are determined from the total energies of a defect supercell E_D^Q by solving the electron chemical potential μ_e from the equation

$$E_D^Q + Q(\mu_e + E_V^Q) = E_D^{Q'} + Q'(\mu_e + E_V^{Q'}). \quad (1)$$

Above, E_V^Q is the position of the valence-band maximum in a defect supercell. The values of E_V^Q for different supercells have been aligned using the average potential corrections.⁶ The obtained defect ionization levels based on the total-energy calculations are given in Table I together with the experimental levels deduced from EPR experiments¹ and positron annihilation spectroscopy measurements.¹⁹ The LSD results agree with the experimental levels well, although the levels lie systematically around 0.2 eV lower in the gap than the experimental values. The underestimation of the band gap typical for LD calculations is possibly reflected in this lowering, especially in the case of the uppermost ionization levels.

The calculations with the Γ point and a supercell of 216 atom sites give a value of 4.94 eV for the formation energy of V_2^0 (Table I). The calculated value for the monovacancy formation energy using the same supercell size and BZ sampling is 3.27 eV.²⁰ This results in a binding energy of 1.60 eV for V_2^0 in excellent agreement with the experimental es-

TABLE II. Calculated distances (d_{ij}) between silicon atoms and relaxation energies (E_r) of a divacancy in different charge states. Results with the Γ -point sampling and the 128- or 216-atom-site supercells are obtained using the VWN parametrization for the exchange and correlation energy. Calculations with the 64-atom-site supercell and with the 2^3 MP mesh use the PZ parametrization. R , P , B , and M denote resonant bond, pairing, inwards breathing, and mixed structures, respectively. G denotes the symmetry point group determined by the ionic structure. XC indicates whether the calculations are spin polarized (LSD) or unpolarized (LD). Distances are given in Å and energies in eV. The ideal distance between the silicon atoms surrounding the divacancy is 3.81 Å.

Defect	XC	Supercell	BZ sampling	d_{12}	d_{13}	d_{23}	d_{45}	d_{46}	d_{56}	G	Type	E_r
V_2^{2+}	LD	216	Γ	3.39	3.38	3.38	3.38	3.38	3.38	D_{3d}	B	0.39
V_2^+	LSD	216	Γ	2.99	3.46	3.41	2.99	3.45	3.41	S_2 ($\sim C_{2h}$)	$M(P)$	0.50
	LSD	128	Γ	3.53	3.70	3.67	3.53	3.70	3.67	S_2 ($\sim C_{2h}$)	$M(P)$	0.19
	LSD	64	2^3	3.17	3.56	3.55	3.17	3.56	3.55	C_{2h}	P	0.33
	LD	64	2^3	3.24	3.52	3.52	3.24	3.52	3.53	C_{2h}	P	
V_2^0	LD	216	Γ	2.89	3.45	3.26	2.89	3.45	3.27	S_2	$M(P)$	0.71
	LD	128	Γ	3.66	3.32	3.46	3.66	3.32	3.46	S_2	$M(R)$	0.31
	LD	64	2^3	3.09	3.43	3.45	3.09	3.43	3.45	S_2 ($\sim C_{2h}$)	P	0.44
V_2^-	LSD	216	Γ	3.38	3.26	3.13	3.38	3.25	3.11	S_2	$M(R)$	0.60
	LSD	128	Γ	3.40	3.53	3.51	3.40	3.53	3.51	S_2 ($\sim C_{2h}$)	P	0.29
	LSD	128	Γ	3.56	3.45	3.44	3.56	3.45	3.44	C_{2h}	R	0.29
	LSD	64	$\Gamma + L$	3.45	3.52	3.55	3.45	3.52	3.55	S_2 ($\sim C_{2h}$)	$M(P)$	
	LSD	64	2^3	3.48	3.04	3.29	3.49	3.28	3.12	C_1 ($\sim C_2$)	M	0.55
	LD	64	2^3	3.30	3.34	3.35	3.29	3.36	3.34	$\sim C_{2h}$	P	0.54
V_2^{2-}	LD	216	Γ	3.23	3.26	3.24	3.23	3.24	3.25	$\sim D_{3d}$	B	0.68
	LD	128	Γ	3.44	3.44	3.43	3.43	3.43	3.44	D_{3d}	B	0.38
	LD	64	2^3	3.29	3.32	3.30	3.31	3.29	3.31	$\sim D_{3d}$	B	0.72

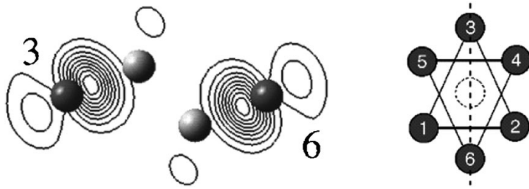


FIG. 2. Spin density $\rho_{\uparrow} - \rho_{\downarrow}$ for the divacancy in the positive charge state. Dark spheres represent atoms, light gray spheres vacancies. The contour spacing is one-tenth of the maximum value (0.055 electrons/ \AA^3). The result is obtained using Γ -point sampling and the 216-atom-site supercell.

estimate of ≈ 1.6 eV given by Watkins and Corbett.¹ Table I also shows results for the other supercell sizes and BZ samplings.

Table II shows the optimized ionic structures and the relaxation energies E_r for V_2 in different charge states. The relaxation energy is defined as the energy difference between the total energies of the ideal and relaxed structures. The energy gain increases considerably with increasing the size of the supercell. The spin polarization increases the energy gain of V_2^+ by 0.03 eV and that of V_2^- by 0.04 eV using the 128-atom-site supercell. Smaller supercells do not allow the defect to relax properly. This phenomenon has been observed also with the silicon monovacancy.²⁰

According to our calculations the doubly positive divacancy V_2^{2+} is not thermodynamically stable for any position of the Fermi level in the band gap. The breathing mode relaxation obtained reflects the fact that there are no electrons in the gap states, and the ionic structure gives a reference against which one can compare the effects of the electrons in the localized defect states.

All our calculations for V_2^+ (one electron in the gap state) give a pairing type relaxation in agreement with the WC model and the EPR experiments¹ as well as with the LD calculation by Saito and Oshiyama.⁴ The LSD calculation with the largest 216-atom-site supercell gives a lower S_2 symmetry but the deviations from the C_{2h} symmetry are small, only about 0.02 \AA . Figure 2 shows the spin density $\rho_{\uparrow} - \rho_{\downarrow}$ in the mirror plane for V_2^+ . The unpaired electron occupies the b_u -type spin orbital and clearly has an amplitude in the approximate mirror plane.

In the neutral charge state V_2^0 the defect states are occupied by two electrons. The calculations with the 216-atom-site supercell result in a *mixed structure* being mainly of the *pairing type* (Table II), in disagreement with the resonant-bond structure found by Seong and Lewis.⁵ The point group symmetry is S_2 in contrast to the C_{2h} symmetry obtained by Seong and Lewis. This discrepancy seems to be due to the defect-defect interactions: The calculation with the 128-atom-site supercell (the defect-defect distance decreased by 1 \AA as compared with the value in the case of the 216-atom-site supercell) results again in a mixed structure but this time it is mainly of the resonant-bond type. The calculations by Seong and Lewis⁵ with a smaller 64-atom-site supercell give the pure resonant bond structure. Also, the increase of the BZ sampling to the 2^3 MP points results in a rather pure pairing state in the case of the 64-atom-site supercell.

The calculations for V_2^- (three electrons in the gap states) with the 216-atom-site supercell result in a *mixed*

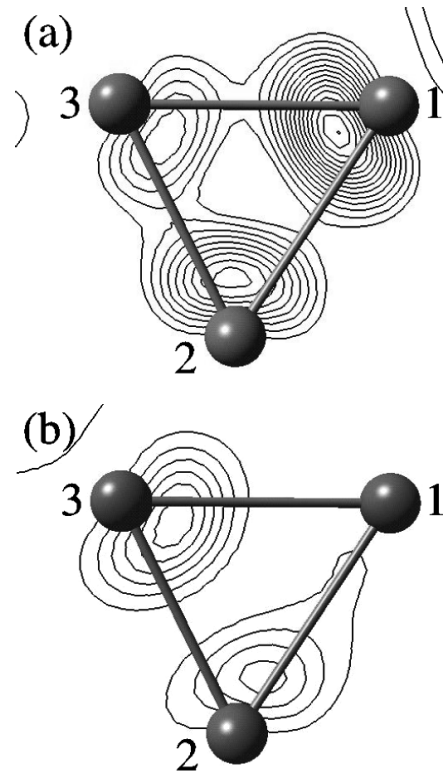


FIG. 3. Defect electron densities of divacancy in the negative charge state obtained using the Γ -point BZ sampling, 216-atom-site supercell and the VWN parametrization. The contour spacing is 0.00387 electrons/ \AA^3 in both figures. (a) Electron density in the two uppermost defect levels that are occupied by three electrons. Contours start from the value 0.0071 electrons/ \AA^3 . (b) Electron density of the uppermost occupied spin orbital. Contours start from the value 0.0009 electrons/ \AA^3 .

structure with an S_2 symmetry (Table II). We argue next that the structure can be classified to a resonant bond type. The defect electron density shown in Fig. 3(a) clearly indicates that it is most natural to place the approximate mirror plane perpendicular to the long d_{12} and d_{56} bonds (and thus such that it includes approximately atoms 3 and 6 and the vacancy sites). The uppermost occupied spin orbital (practically $\rho_{\uparrow} - \rho_{\downarrow}$) shown in Fig. 3(b) has the highest value near atom 3 (and 6) and therefore on the approximate mirror plane of the defect. It is this maximum that gives rise to the main EPR and electron-nuclear double resonance signals. Thus this structure agrees better with the resonant bond result obtained by Saito and Oshiyama⁴ than with the WC model. However, the S_2 symmetry does not seem to agree with the EPR experiment.¹ S_2 belongs to the triclinic system whereas the $G7$ spectrum by Watkins and Corbett¹ corresponds to the monoclinic- I system.²¹ The reason for this discrepancy is presently not clear to us. The S_2 symmetry is obtained from a well-converged calculation and we do not expect any further refinements to change this symmetry. Some possible explanations are as follows: (i) A motional averaging smoothing the difference between d_{13} and d_{23} as well as d_{46} and d_{56} may be present already at low temperatures ($T < 10$ K), with the effect of raising the effective symmetry from S_2 to C_{2h} , (ii) the quantum-mechanical zero point motion of the nuclei—not included in the LSD calculations—may contribute in raising the effective symmetry, (iii) the experimental

resolution may not be sufficient to fully distinguish small differences between S_2 and C_{2h} .²²

As to the bonding, the uppermost occupied spin orbital is antibonding for atoms 2 (5) and 3 (6) [change of the sign between the atoms, Fig. 3(b)] increasing the shortest bond lengths from 2.89 to 3.11–3.13 Å (Table II). On the other hand, the largest lengths decrease from 3.45 to 3.38 Å indicating that this spin-orbital is bonding between atoms 2 (5) and 1 (4).

The calculations for V_2^{2-} (four electrons in the gap states) result in a rather symmetric inwards breathing mode structure with an approximate D_{3d} symmetry (Table II). This is as expected: the JT mechanism does not lower the total energy because the degenerate e_u state is now fully occupied by four electrons.

In conclusion, well-converged, fully relaxed LSD calculations give for the charged and neutral divacancy in Si formation and binding energies as well as ionization levels that agree quite closely with experiments. We find that positively charged, neutral, and negatively charged divacancies have mixed structures of the S_2 symmetry that are lower in energy than those of the C_{2h} symmetry. The structures of the positive and neutral divacancies are of the pairing type whereas the negatively charged divacancy is of the resonant bond type, in agreement with Saito and Oshiyama.

We acknowledge the generous computing resources of the Center for Scientific Computing (CSC), Espoo, Finland. We want to thank M. J. Puska, J. Eloranta, and R. Laiho for fruitful discussions.

-
- ¹G. D. Watkins and J. W. Corbett, Phys. Rev. A **138**, A543 (1965).
²G. D. Watkins, in *Deep Centers in Semiconductors*, edited by S. T. Pantelides (Gordon and Breach, New York, 1986), pp. 147–183.
³O. Sugino and A. Oshiyama, Phys. Rev. B **42**, 11 869 (1990).
⁴M. Saito and A. Oshiyama, Phys. Rev. Lett. **73**, 866 (1994).
⁵H. Seong and L. J. Lewis, Phys. Rev. B **53**, 9791 (1996).
⁶S. Pöykkö, M. J. Puska, and R. M. Nieminen, Phys. Rev. B **53**, 3813 (1996).
⁷G. D. Watkins, Phys. Rev. Lett. **74**, 4353 (1995).
⁸M. Saito and A. Oshiyama, Phys. Rev. Lett. **74**, 4354 (1995).
⁹O. Gunnarsson, B. L. Lundqvist, and J. W. Wilkins, Phys. Rev. B **10**, 1319 (1974); O. Gunnarsson and B. I. Lundqvist, *ibid.* **13**, 4274 (1976).
¹⁰S. H. Vosko, L. Wilk, and M. Nusair, Can. J. Phys. **58**, 1200 (1980).
¹¹J. Perdew and A. Zunger, Phys. Rev. B **23**, 5048 (1981).
¹²D. M. Cerperley and B. J. Alder, Phys. Rev. Lett. **45**, 566 (1980).
¹³In the spin-unpolarized case the VWN LD approximation essentially coincides with the PZ LD approximation. Both parametrizations use the same exchange part and the difference comes from the correlation part.
¹⁴D. R. Hamann, Phys. Rev. B **40**, 2980 (1989); M. Fuchs and M. Scheffler (unpublished).
¹⁵L. Kleinman and D. M. Bylander, Phys. Rev. Lett. **48**, 1425 (1982).
¹⁶S. G. Louie, S. Froyen, and M. L. Cohen, Phys. Rev. B **26**, 1738 (1982).
¹⁷H. J. Monkhorst and J. D. Pack, Phys. Rev. B **13**, 5188 (1976).
¹⁸See Appendix A in S. Pöykkö, M. J. Puska, and R. M. Nieminen, Phys. Rev. B **57**, 12 174 (1998), and references therein.
¹⁹P. Hautojärvi, K. Saarinen, J. Mäkinen, and C. Corbel, Defect Diffus. Forum **153-155**, 97 (1998); H. Kauppinen, C. Corbel, J. Nissilä, K. Saarinen, and P. Hautojärvi, Phys. Rev. B **57**, 12 911 (1998).
²⁰M. J. Puska, S. Pöykkö, M. Pesola, and R. M. Nieminen, Phys. Rev. B **58**, 1318 (1998).
²¹C. A. J. Ammerlaan, in *Numerical Data and Functional Relations in Science and Technology*, edited by O. Madelung and M. Schulz, Landolt-Börnstein, New Series, Group III, Vol. 22, Pt. b (Springer-Verlag, Berlin, 1989), p. 365.
²²J. Eloranta and R. Laiho (private communication).